

## **SUPPLEMENTARY INFORMATION**

### **Bright Future for Steam Reforming of Methane: Highly Efficient Visible Light Photocatalysis**

Bing Han,<sup>a</sup> Wei Wei,<sup>a</sup> Meijia Li,<sup>a</sup> Kai Sun,<sup>b</sup> and Yun Hang Hu<sup>a\*</sup>

a. Department of Materials Science and Engineering, Michigan Technological University, 1400  
Townsend Drive, Houghton, MI 49931-1295, USA

b. Department of Materials Science and Engineering, University of Michigan, Ann Arbor, MI,  
48109-2136, USA.

## **CONTENT:**

### **1. Experimental section**

### **2. Thermodynamic equilibrium calculations**

- **Table S1** (*The thermodynamic equilibrium of steam reforming of CH<sub>4</sub>*)

### **3. Band potential measurement of black TiO<sub>2</sub>**

### **4. SEM image and UV-visible light absorption**

- **Figure S1** (*FESEM image of Pt/blackTiO<sub>2</sub> coated on SiO<sub>2</sub> substrate*)
- **Figure S2** (*UV-Visible spectra of Pt/blackTiO<sub>2</sub> and white TiO<sub>2</sub> on SiO<sub>2</sub> substrate*)

### **5. Photocatalytic reactor**

- **Figure S3** (*Photocatalytic reactor*)

## 6. Thermal images of catalysts

- **Figure S4** (*Thermal images of Pt/blackTiO<sub>2</sub> catalyst dispersed on a SiO<sub>2</sub> substrate*)

## 7. Steam reforming of methane over Pt/Al<sub>2</sub>O<sub>3</sub>

- **Figure S5** (*H<sub>2</sub>, CO, and CO<sub>2</sub> yields over Pt/Al<sub>2</sub>O<sub>3</sub> with and without light illumination*)

## 8. Photocatalytic steam reforming of methane over Pt/BlackTiO<sub>2</sub>

- **Figure S6** (*Photo product yields vs. incident visible light energy*)

## 9. Calculation detail of the apparent quantum efficiency (QE)

- **Table S2** (*Photo hydrogen yields and QE*)

## 10. Temperature-dependence of TiO<sub>2</sub> band gap

- **Figure S7** (*UV-Visible spectra at elevated temperatures, relationship between energy gap and temperature, and XRD patterns of TiO<sub>2</sub>*)

## 11. Catalyst characterization

- **Figure S8** (*TEM, XPS, XRD, and EPR characterization*)

## **1. EXPERIMENTAL SECTION**

**Pt/blackTiO<sub>2</sub> catalyst and its dispersion on light-diffuse-reflection-surface:** The method of catalyst preparation, which is the same as used in our previous work,<sup>1</sup> is described as follows: (1) 1wt% Pt/TiO<sub>2</sub> catalyst was synthesized by impregnating TiO<sub>2</sub> powder (Degussa P25 with surface area of 48 m<sup>2</sup>/g) in aqueous solution of H<sub>2</sub>PtCl<sub>6</sub>·6H<sub>2</sub>O at 25 °C overnight, followed by calcination at 500 °C for 2 hours. The obtained Pt/TiO<sub>2</sub> powder, which was located in a ceramic tube reactor (diameter of 3 cm), was vacuumed for 6 hours. Then, hydrogen was introduced into the reactor, followed by increasing temperature to 200 °C in 20 min and remaining the temperature for 24 hours. Consequently, Pt/blackTiO<sub>2</sub> catalyst was generated. (2) SiO<sub>2</sub> substrate was prepared as follows: Silicon dioxide and quartz wool were mixed with water at weight ratio of 30:30:1 and then heated to 1100 °C for 2h to form a piece of white solid. The solid piece was shaped as a rectangle disk substrate (1.4 cm × 2.9 cm). Its excellent light scattering properties were demonstrated using Shimadzu UV-Vis spectrophotometer. (3) Pt/blackTiO<sub>2</sub> catalyst was dispersed on light-diffuse-reflection-surface by mixing Pt/blackTiO<sub>2</sub> powder with water as a paste, followed by coating on the surface of the SiO<sub>2</sub> substrate and then drying at 25 °C overnight. The description of catalyst characterization was described in the supporting information.

**Photocatalytic reaction test:** Pt/blackTiO<sub>2</sub> catalyst (15 mg) on the light-diffuse-reflection-surface of a SiO<sub>2</sub> rectangle disk substrate (1.4 cm × 2.9 cm) was located in a quartz tubular flow reactor (diameter: 1.5 cm). To carry out PSRM, the reactor was heated to a selected temperature by an electrical furnace. Deionized water was injected into flowing CH<sub>4</sub> stream (flow rate = 10 ml/min) by a syringe pump (Cole Parmer) and vaporized and homogenized with gas feed before entering the reactor. To eliminate the effect of light illumination on the temperature of catalyst, an *in-situ* thermocouple in contact with sample was employed for accurate temperature-control. The catalyst

was irradiated by 150 W Xenon lamp coupled with 1.5 G light filter (100 mW/cm<sup>2</sup>, Newport solar simulator) with irradiation area of 4 cm<sup>2</sup>. For visible light photocatalytic reaction test, UV light filter was employed to block UV (wavelength < 420 nm) light in the simulated sunlight. Argon was exploited to carry gas products into on-line gas chromatograph (GC) equipped with a Porapak Q column and a 5A column for composition analysis. Furthermore, the condensed liquid products were analyzed by GC-MS. The measurements showed that products were H<sub>2</sub>, CO, and CO<sub>2</sub>. No other products were detected.

**Apparent quantum efficiency:** In photocatalytic steam reforming of methane, the reduction reaction is water (H<sub>2</sub>O and CH<sub>4</sub>) to H<sub>2</sub>, whereas CH<sub>4</sub> to CO<sub>2</sub> (and/or CO) is an oxidation reaction. Because the production of each H<sub>2</sub> molecule from H<sub>2</sub>O or CH<sub>4</sub> requires 2 electrons via the reduction process, the apparent quantum efficiency (QE) can be expressed as follows:

$$QE = \frac{(\text{number of photo } H_2) \times 2}{\text{number of incident photons}} \quad (1)$$

The measurements of incident photons were carried out using Newport Quantum Efficiency Test Instrument under the same illuminations (visible light or AM 1.5 G sunlight) as used for the photocatalytic reactions (Please see the Supplementary Information for QE calculation details).

## **2. THERMODYNAMIC EQUILIBRIUM CALCULATIONS**

The thermodynamic equilibrium of steam reforming of CH<sub>4</sub> (SRM) was calculated and results were listed in Table S1. One can see that high equilibrium conversions of reactants need a high temperature, whereas a high selectivity for 4H<sub>2</sub>+CO<sub>2</sub> without CO (Equation 3: H<sub>2</sub>O + CH<sub>4</sub> → 4H<sub>2</sub> + CO<sub>2</sub>) requires a low reaction temperature (Table S1).

**Table S1.** The thermodynamic equilibrium of steam reforming of CH<sub>4</sub>

<b>T (K)</b>	<b>Reactant Conversion (%)</b>		<b>Product Selectivity (%)</b>		
	<b><i>H<sub>2</sub>O</i> (%)</b>	<b><i>CH<sub>4</sub></i> (%)</b>	<b><i>H<sub>2</sub></i> (%)</b>	<b><i>CO</i> (%)</b>	<b><i>CO<sub>2</sub></i> (%)</b>
300	0.010	0.005	80.000	0.000	20.000
400	0.144	0.288	80.000	0.000	20.000
500	1.130	2.260	79.999	0.007	19.995
600	4.570	9.108	79.972	0.141	19.887
700	12.380	23.970	79.741	1.293	18.965
800	26.930	45.693	78.709	6.457	14.834
900	52.170	67.828	76.745	16.275	6.980
1000	78.930	85.240	75.490	22.550	1.960
1100	92.440	94.269	75.123	24.385	0.492
1200	97.170	97.718	75.035	24.824	0.141
1300	98.810	98.998	75.012	24.940	0.048
1400	99.440	99.514	75.005	24.977	0.018
1500	99.710	99.743	75.002	24.990	0.008

### **3. BAND POTENTIAL MEASUREMENT OF BLACK TiO<sub>2</sub>**

The band potential measurement of black TiO<sub>2</sub> was reported in our previous work.<sup>[18]</sup> It is briefly described as follows: **(1)** Electron paramagnetic resonance (EPR) measurements were carried out for pristine (white) TiO<sub>2</sub>, Pt/nonblackTiO<sub>2</sub>, and Pt/blackTiO<sub>2</sub>. It was found that the peak intensity of Ti<sup>3+</sup> is very small for white TiO<sub>2</sub> and unreduced Pt/TiO<sub>2</sub>, indicating their negligible amount of Ti<sup>3+</sup>. In contrast, the Pt/blackTiO<sub>2</sub> exhibits a large amount of Ti<sup>3+</sup> associated with a large peak of Ti<sup>3+</sup>. **(2)** The Fourier transform near infrared (FT-NIR) spectrum of the Pt/black/TiO<sub>2</sub> (prepared by hydrogenation) was determined using a Bomem (MB 160) Fourier transform near infrared spectrophotometer in the wavenumber range 4000-11000 cm<sup>-1</sup> at room temperature. The spectra show that Pt/blackTiO<sub>2</sub> exhibited strong absorption in the wavenumber range of 4000-11000 cm<sup>-1</sup>, whereas obvious absorption was not observed for white TiO<sub>2</sub> and Pt/non-blackTiO<sub>2</sub> (without hydrogenation). Furthermore, the calculated energy gap from the FT-NIR spectra is 1.3 eV. In contrast, white TiO<sub>2</sub> and Pt/non-blackTiO<sub>2</sub> don't absorb light in the wavenumber range of 4000-11000 cm<sup>-1</sup>. Because Ti<sup>3+</sup> is present in the Pt/blackTiO<sub>2</sub> (not in white TiO<sub>2</sub> and Pt/non-blackTiO<sub>2</sub>), an energy gap of 1.3 eV of the Pt/blackTiO<sub>2</sub> would be due to the Ti<sup>3+</sup> donor level. Namely, the energy gap between the conduction band (CB) and the generated donor level (Ti<sup>3+</sup>) for Pt/blackTiO<sub>2</sub> is 1.3 eV. **(3)** Band edge potentials (E<sub>cb</sub>) of pristine (white) TiO<sub>2</sub>, Pt/non-blackTiO<sub>2</sub>, and the Pt/blackTiO<sub>2</sub> catalyst were calculated from flat-band potentials (E<sub>fb</sub>) (determined by Mott-Schottky method). The valence band edge potential (E<sub>vb</sub>) was obtained by combining the conduction band edge potential with the VB-CB energy gap.

#### 4. SEM IMAGE AND UV-VISIBLE LIGHT ABSORPTION

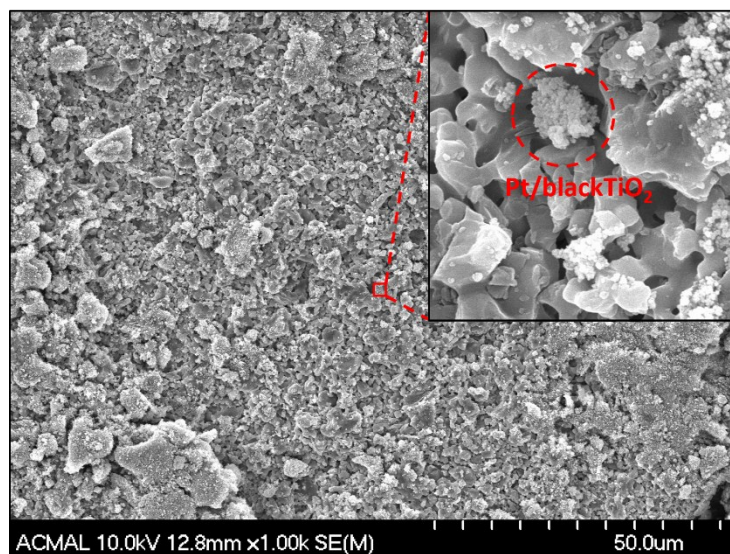


**Figure S1.** FESEM image of Pt/blackTiO<sub>2</sub> coated on the SiO<sub>2</sub> substrate.

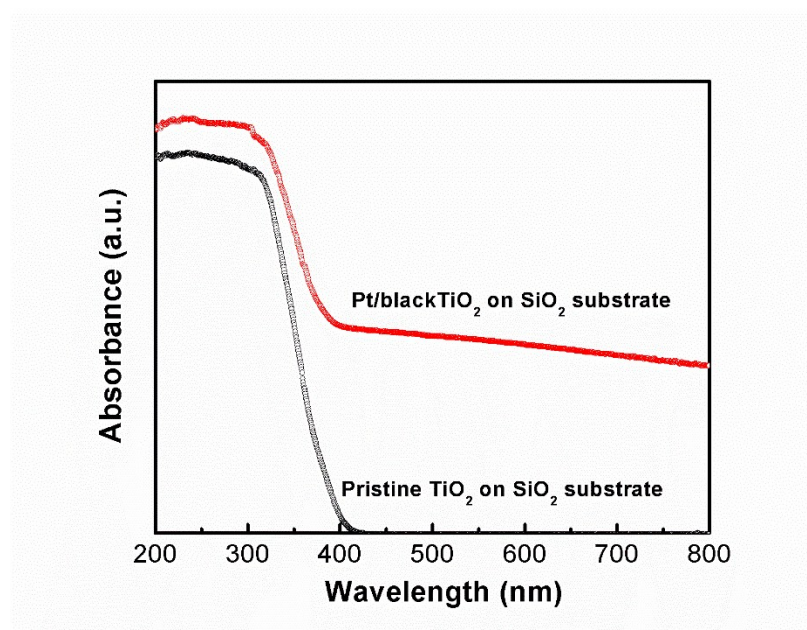


**Figure S2.** UV-Visible spectra of Pt/blackTiO<sub>2</sub> and white TiO<sub>2</sub> on the SiO<sub>2</sub> substrate.

## 5. PHOTOCATALYTIC REACTOR

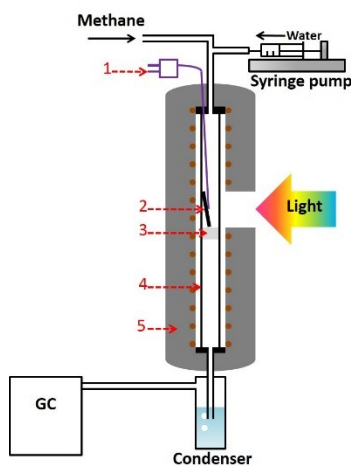


**Figure S3.** Test unit schematic for photocatalytic steam reforming of methane. (1) Thermocouple, (2) Pt/blackTiO<sub>2</sub> on the SiO<sub>2</sub> substrate, (3) Quartz wool, (4) Quartz tube reactor, and (5) Electrical tube furnace.

## 6. THERMAL IMAGES OF CATALYSTS

AM 1.5G sunlight (a weak light: 100mW/cm<sup>2</sup>) illumination on catalyst would be unable to cause a large temperature increase and hot spots for catalyst bed. To obtain direct evidences for proving this, we employed a high performance thermal imager (CEM, DT-980H CEM, DT-980H) to acquire thermal images for the Pt/black TiO<sub>2</sub> dispersed on SiO<sub>2</sub> substrate. As shown in Fig.S1, one can see that the catalyst temperature without light irradiation is uniform with 0.7~5.9 °C difference between maximum and minimum temperatures at various furnace setting temperatures. Under light irradiation, the average temperature of the catalyst increased by only 4.7~8.1°C. Furthermore, the temperature of the catalyst with light irradiation is also uniform just with 0.6~3.7°C difference between maximum and minimum



temperatures. This clearly demonstrated that the light irradiation didn't create hot spots on the catalyst. Furthermore, the light-increased temperature is small (8.1 °C or less).

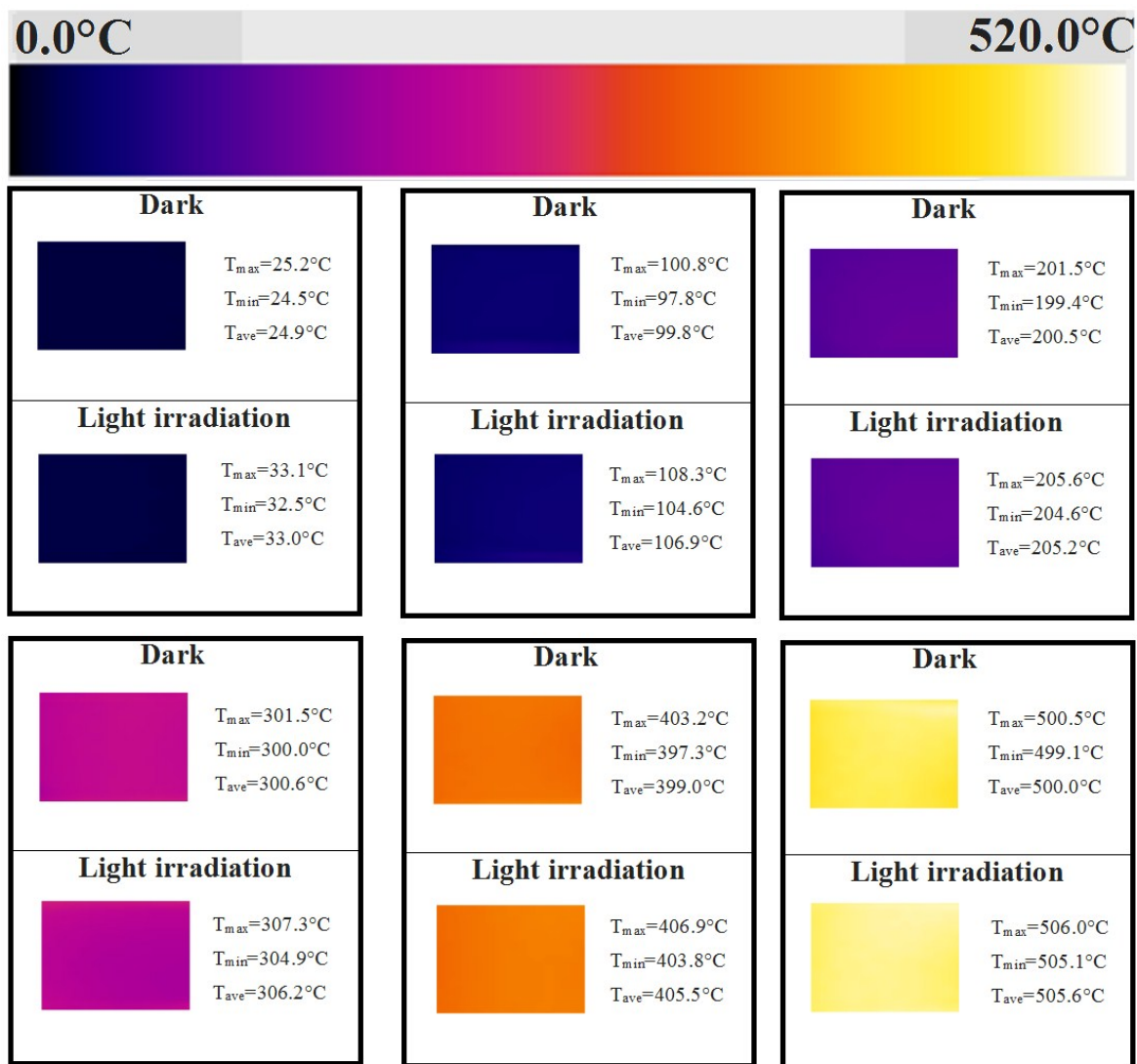
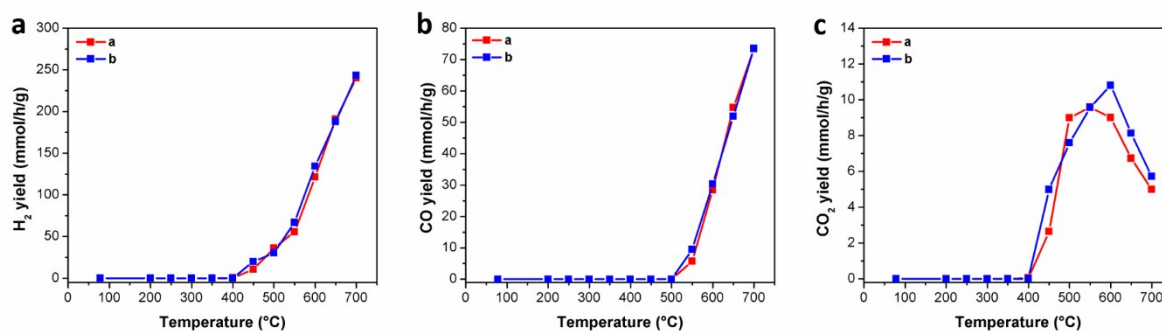


Figure S4. Thermal images of Pt/blackTiO<sub>2</sub> catalyst dispersed on a SiO<sub>2</sub> substrate with a high performance thermal imager (CEM, DT-980H) under dark and light irradiation (AM 1.5G, 100mW/cm<sup>2</sup>) at various furnace setting temperatures. (The IR sensor resolution of the instrument is 80x80 pixels).

## 7. STEAM REFORMING OF METHANE OVER Pt/Al<sub>2</sub>O<sub>3</sub>



**Figure S5.** H<sub>2</sub>, CO, and CO<sub>2</sub> yields from steam reforming of methane (water/CH<sub>4</sub> molar ratio=1:1 and GHSV=80000 ml/gcat/h) over 1 wt% Pt/Al<sub>2</sub>O<sub>3</sub> catalyst dispersed on the light-diffuse-reflection-surface of the SiO<sub>2</sub> substrate (a-AM 1.5 G illumination, b-without light illumination).

## 8. PHOTOCATALYTIC STEAM REFORMING OF METHANE OVER Pt/TiO<sub>2</sub>

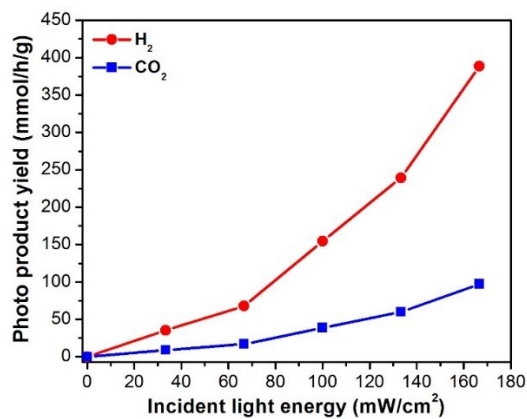


**Figure S6.** Photo product yields vs. incident light energy under  $\lambda > 420$  nm visible light (450°C, water/CH<sub>4</sub> molar ratio 1:1 and GHSV=80000 ml/h/gcat) for steam reforming of methane over Pt/BlackTiO<sub>2</sub> dispersed on light-diffuse-reflection-surface of a SiO<sub>2</sub> substrate.

## **9. CALCULATION OF APPARENT QUANTUM EFFICIENCIES**

In photocatalytic steam reforming of methane, the oxidation of CH<sub>4</sub> to CO<sub>2</sub> and CO requires 8 and 6 electrons, respectively, while the reduction of water (H<sub>2</sub>O and CH<sub>4</sub>) to H<sub>2</sub> requires 2 electrons. We have two methods to calculate the apparent quantum efficiency (QE) via reduction and oxidation reactions:

(1) According to reduction reaction, QE can be expressed as

$$QE = \frac{(\text{number of photo } H_2) \times 2}{\text{number of incident photons}} \quad (4)$$

(2) Based on oxidation reduction, QE can be calculated as

$$QE = \frac{(\text{number of photo CO yield}) \times 6 + (\text{number of photo CO}_2 \text{ yield}) \times 8}{\text{number of incident photons}} \quad (5)$$

The detail calculation for QE is shown as follows: When simulated visible light irradiates 4cm<sup>2</sup> area of the catalyst system with 0.015g Pt/blackTiO<sub>2</sub> catalyst, the introduced photon number, which was measured by Newport Quantum Efficiency Test Instrument, is 5.46x10<sup>21</sup> h<sup>-1</sup>. At 500 °C, the produced photo hydrogen is 2.7218 mmol/h. Therefore, we can obtain the number of produced photo hydrogen molecules (N<sub>H2</sub>):

$$N_{H_2} = (2.7218 \times 0.001) \times (6.0221 \times 10^{23}) = 1.6391 \times 10^{21} h^{-1}$$

With Equation 4, QE can be calculated as:

$$QE = \frac{(1.691 \times 10^{21}) \times 2}{5.46 \times 10^{21}} \times 100\% = 60.0\%$$

Furthermore, we also used the products (CO and CO<sub>2</sub>) of oxidation to calculate the QE with Equation S1, leading to QE of 61.3% at 500°C, which is very close to the QE value of 60.0% from H<sub>2</sub> production. Therefore, QE at various temperatures were calculated from produced photo H<sub>2</sub> numbers with Equation 4 and listed in Table S2.

**Table S2.** Photo hydrogen yields and the apparent quantum efficiencies from photocatalytic SRM over 0.015g Pt/BlackTiO<sub>2</sub> catalyst:

	<b>AM 1.5G Light</b>		<b>Visible Light</b>	
<b>T(°C)</b>	<b>Photo H<sub>2</sub></b> Yield (mmol/h)	<b>QE</b> (%)	<b>Photo H<sub>2</sub></b> Yield (mmol/h)	<b>QE</b> (%)
200	0.0039	0.1	0.0000	0.0
250	0.0412	0.9	0.0020	0.1
300	0.1140	2.5	0.0291	0.6
350	0.2945	6.5	0.2146	4.7
400	0.9844	21.7	0.8860	19.5
450	2.3390	51.6	2.2194	49.0
500	2.9281	64.6	2.7218	60.0

## **10. TEMPERATURE-DEPENDENCE OF TiO<sub>2</sub> BAND GAP**

UV-Visible spectra of TiO<sub>2</sub> were obtained at various temperatures (25-370 °C). As shown in Fig. S7a, one can see a small difference in the UV-Visible spectra obtained at different temperatures. Furthermore, we calculated band gaps from the spectra, and then plotted it with temperature (Fig.7b). It can be seen that the band gap slightly and linearly decreased with increasing temperature. Namely, when temperature was changed by 345 °C (from 25 to 370 °C), only 0.109eV decrease in band gap (from 3.046 to 2.937 eV) was observed. Based on the obtained linear relationship between band gap and temperature, we calculated the band gap of 2.908 eV at 500 °C. This indicates that only 0.138 eV in band gap was decreased by increasing temperature from 25 to 500 °C. This small decrease in TiO<sub>2</sub> band gap was further supported by high temperature XRD measurements. Fig. S6c shows that its XRD pattern remained unchanged with increasing temperature from room temperature to 500 °C. This indicates that interatomic spaces in TiO<sub>2</sub> remained almost unchanged with increasing temperature. It was reported that the energy bandgap of semiconductors tends to decrease with increasing temperature, which is due to interatomic spacing increases (<https://ecee.colorado.edu/~bart/book/eband5.htm>). Therefore, with increasing temperature from 25 to 500 °C, the unchanged interatomic spaces (Fig. S7c) support a very little change of band gap for TiO<sub>2</sub> (Fig. S7a and b).

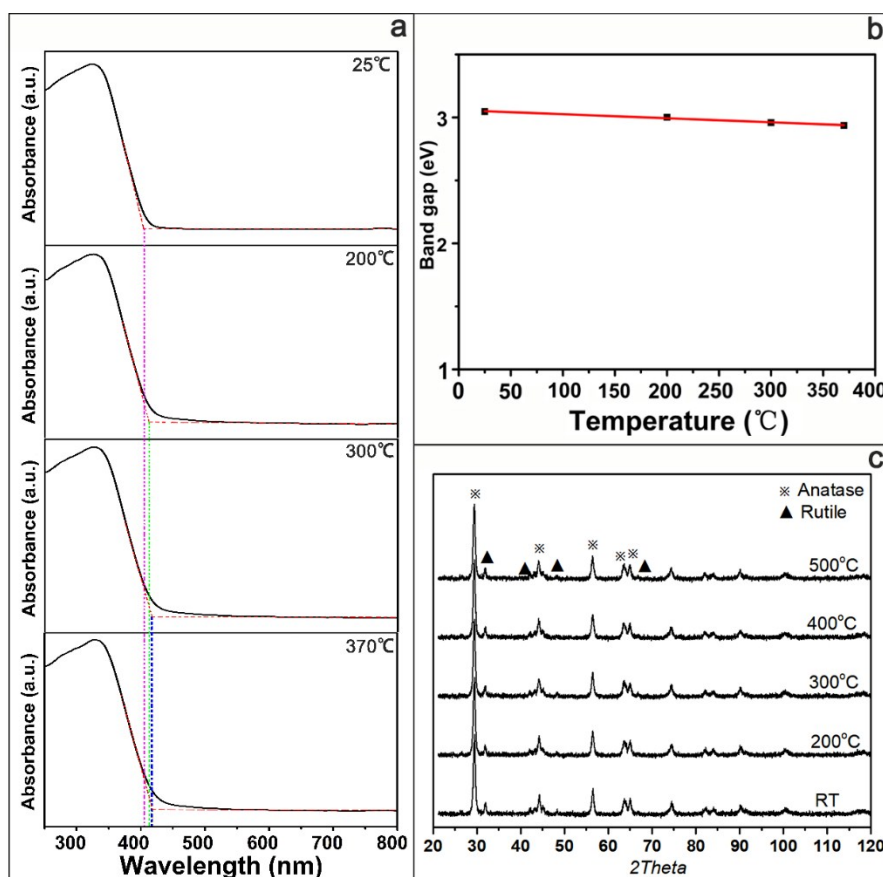


**Figure S7.** (a). UV-vis absorbance spectra of TiO<sub>2</sub> at various temperatures; (b). The band gap of TiO<sub>2</sub> vs. temperature; (c). XRD patterns of TiO<sub>2</sub> at various temperatures.

## **11. CATALYST CHARACTERIZATION**

The 1wt% Pt/BlackTiO<sub>2</sub> catalyst was examined by X-ray diffraction (XRD) using a Scintag XDS-2000 powder diffract meter with Cu K $\alpha$  ( $\lambda=1.5406\text{\AA}$ ) radiation. Its dispersion on SiO<sub>2</sub> substrate was characterized by Hitachi-4700 field emission scanning electron microscope (FESEM) with energy dispersive spectroscopy (EDS). The microstructure of the catalyst was

evaluated using JEOL JEM-3100R05 transmission electron microscope (TEM). X-ray photoelectron spectra (XPS) were collected using a Kratos Ultra AXIS DLD XPS with a monochromated Al source. Electron paramagnetic resonance (EPR) spectra of the catalyst were recorded at 77K by a commercial continuous wave (CW) X-band (9-10 GHz) EPR spectrometer ESP-300E from Bruker.

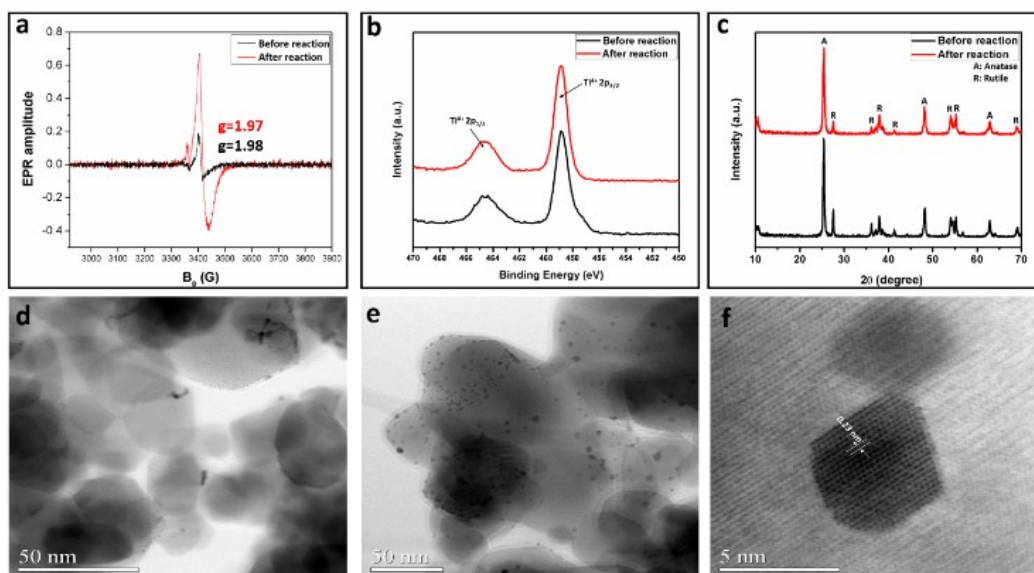


Fig. S8 Characterization of Pt/BalckTiO<sub>2</sub> catalyst: (a) 77K Electron paramagnetic resonance (EPR) spectra, (b) X-ray photoelectron spectra (XPS), (c) X-ray diffraction (XRD) patterns, (d) Transmission Electron Microscopy (TEM) image before the reaction, (e) TEM image after the reaction, and (f) high resolution TEM image after the reaction (note: the reaction is the photocatalytic steam reforming for 30 hours under visible light illumination at 500 °C).

Reference:

1. B. Han, W. Wei, L. Chang, Y. H. Hu, *ACS Catal.*, 2016, **6**, 494-497.